Locally Generated Tsunamis Recorded on the Coast of British Columbia

Alexander B. Rabinovich[1,2], Richard E. Thomson[1,*], Vasily V. Titov[3], Fred E. Stephenson[4] and Garry C. Rogers[5]

[1]*Department of Fisheries and Oceans*
Ocean Sciences Division
Institute of Ocean Sciences
9860 West Saanich Road
Sidney BC V8L 4B2

[2]*Russian Academy of Sciences*
P.P. Shirshov Institute of Oceanology
Moscow, Russia

[3]*National Oceanic and Atmospheric Administration*
Pacific Marine Environmental Laboratory
Seattle, WA USA

[4]*Department of Fisheries and Oceans*
Canadian Hydrographic Service, Institute of Ocean Sciences
Sidney BC

[5]*Natural Resources Canada*
Geological Survey of Canada, Pacific Geoscience Centre
Sidney BC

[Original manuscript received 18 June 2007; accepted 12 February 2008]

ABSTRACT *This study presents analyses and numerical simulations of local tsunamis generated by two recent earthquakes off the coast of British Columbia. The Queen Charlotte Islands earthquake (M_w = 6.1) on 12 October 2001 generated waves that were recorded by tide gauges at Bamfield, Tofino, Winter Harbour and Port Hardy on the coast of Vancouver Island, with maximum measured wave heights of 11.3, 18.2, 22.7 and 14.5 cm, respectively. The Explorer Plate earthquake off Vancouver Island (M_w = 6.6) on 2 November 2004 generated waves recorded only at Bamfield and Tofino, with lower heights of 7.5 cm and 10.8 cm, respectively. The generation of tsunamis by these moderate, M_w = 6.1–6.6, local earthquakes suggests the possibility of destructive tsunamis from local sources other than the Cascadia Subduction Zone. This, in turn, has implications for tsunami hazards for this seismically active region of coastal North America.*

RÉSUMÉ *[Traduit par la rédaction] Cette étude présente les analyses et la simulation numérique de tsunamis locaux produits par deux récents tremblements de terre au large des côtes de la Colombie-Britannique. Le tremblement de terre des îles de la Reine-Charlotte (M_w = 6,1), le 12 octobre 2001, a produit des vagues qui ont été enregistrées par des marégraphes à Bamfield, Tofino, Winter Harbour et Port Hardy sur la côte de l'île de Vancouver, avec des hauteurs de vagues maximales mesurées de 11,3, 18,2, 22,7 et 14,5 cm, respectivement. Le tremblement de terre de la plaque Explorer au large de l'île de Vancouver (M_w = 6,6), le 2 novembre 2004, a produit des vagues enregistrées seulement à Bamfield et Tofino, avec de plus faibles hauteurs, de 7,5 et 10,8 cm, respectivement. La production de tsunamis par ces tremblements de terre locaux d'intensité modérée (M_w = 6,1–6,6) suggère la possibilité de tsunamis destructeurs de sources locales autres que la zone de subduction Cascadia. Cela en retour donne à entrevoir les dangers liés aux tsunamis dans cette région d'activité sismique de l'Amérique du Nord côtière.*

*Corresponding author's e-mail: Richard.Thomson@dfo-mpo.gc.ca

1 Introduction

The magnitude $M_w = 9.3$ earthquake that occurred offshore of Sumatra on 26 December 2004 generated highly destructive tsunami waves that severely damaged the coastal regions of the Indian Ocean and killed more than 226,000 people. Waves from this event were recorded around the world, revealing the unprecedented global reach of the 2004 tsunami (Titov et al., 2005b; Rabinovich et al., 2006a). Because of international tourism, many countries far removed from the major disaster areas lost citizens, triggering widespread scientific and public interest in this catastrophic event and in tsunamis in general.

A common concern for specialists and the public alike is whether other coastal regions are also vulnerable to similar disastrous tsunamis. The coast of British Columbia, extending from approximately 48°N to 55°N with a net length (including inlets, straits, passes, sounds, and narrows) of approximately 27,300 km (Thomson, 1981), is especially susceptible to damage from tsunamis generated within the Pacific basin (Rapatz and Murty, 1987; Murty, 1992). Until recently, there have been no numerical models to simulate tsunamis effectively in real-time. Such models now exist (Whitmore, 2003; Titov et al., 2005a). These models are also useful for diagnostic purposes, including global catastrophic events such as the 2004 Sumatra tsunami (Titov et al., 2005b; Kowalik et al., 2007). A major threat for the coast of British Columbia (BC) are Cascadia Subduction Zone (CSZ) earthquakes (Murty, 1992; Clague, 2001). The last known Cascadia earthquake ($M = 9.0$–9.3) was on 26 January 1700 (Atwater et al., 2005). Tsunami waves from this earthquake crossed the Pacific and struck the coast of Japan with wave heights up to several metres (Satake et al., 1996, 2003). Similar catastrophic waves could be generated by a future CSZ megathrust earthquake. Cherniawsky et al. (2007) used several rupture scenarios for such potential earthquakes in numerical experiments to study the propagation of tsunami waves off the west coast of North America and to predict tsunami wave heights in several bays and harbours on southern Vancouver Island, typically in the range of 4 to 15 m. However, because no observational data exist for this event, the model results provide only unverified preliminary estimates.

Geological and geophysical evidence collected along the western coastline of Vancouver Island, as well as on the Washington and Oregon coasts, show that major Cascadia earthquakes accompanied by destructive tsunamis have an average recurrence interval of approximately 500 years (Adams, 1990; Clague and Bobrowsky, 1999; Clague et al., 2003). Trans-Pacific tsunamis generated by major earthquakes along the Pacific 'Rim of Fire' (which includes the Aleutian, Kuril-Kamchatka, Japanese, Indonesian, Philippine, and Chilean seismic zones) can also significantly affect the BC coast (Murty, 1992; Clague, 2001). The 1964 Alaska ('Good Friday') earthquake with a magnitude $M_w = 9.2$ triggered a catastrophic tsunami which swept southward from the source area near Prince William Sound, Alaska, to the BC coast where it caused roughly Can$10 million damage (1964 dollars) (Wigen and White, 1964; Murty, 1977; Clague, 2001). According to Rapatz and Murty (1987) and Murty (1992), the west coast of Canada may also be highly susceptible to devastating tsunamis caused by local earthquakes with source areas located offshore from northern Vancouver Island and the Queen Charlotte Islands.

The lack of reliable observational tsunami data is a key factor limiting our ability to estimate tsunami risk and to verify existing numerical tsunami models for the west coast of Canada. Wigen (1983) reviewed analogue tide gauge records for Tofino for responses to 1450 earthquakes recorded from 1905 to 1980 and identified 43 tsunamis for the coast of BC All 43 tsunamis were associated with distant earthquakes. The two largest tsunamis noted by Wigen (1983) were those due to the $M_w = 9.2$, 1964 Alaskan earthquake (2.40 m) and the $M_w = 9.5$, 1960 Chilean earthquake (1.26 m).

The destructive tsunamis of the 1990s in the Pacific Ocean initiated a major upgrade of the existing Tsunami Warning and Permanent Water Level Network (PWLN) stations on the coast of BC. The new precise digital instruments were designed to measure sea level variations continuously with one-minute sampling. During the period 1999–2007, long-term series of high quality one-minute sea level data were collected and nine weak tsunamis were recorded, including the Peru tsunami of 23 June 2001 (Rabinovich and Stephenson, 2004), the Great Sumatra tsunami of 26 December 2004 (Rabinovich et al., 2006a), the California tsunami of 15 June 2005 (Rabinovich et al., 2006b), and the Simushir (Central Kuril Islands) tsunamis of 15 November 2006 and 13 January 2007 (Rabinovich et al., 2008). In particular, the 2004 Sumatra tsunami was identified at six tide gauges located on the outer BC coast. These sites (and their maximum recorded wave heights) are Victoria (11.7 cm), Bamfield (4.5 cm), Tofino (15.4 cm), Winter Harbour (21.0 cm), Port Hardy (4.5 cm) and Bella Bella (9.0 cm) (Rabinovich et al., 2006a).

Two of the nine tsunamis observed using the new digital instruments were generated by local earthquakes, and appear to be the first local tsunamis ever instrumentally recorded on this coast. The Queen Charlotte Islands (QCI) tsunami of 12 October 2001 was generated by a moderate $M_w = 6.1$ earthquake on the continental slope (Fig. 1). Tsunami waves from this event were recorded by four tide gauges on the coast of Vancouver Island: Port Hardy, Winter Harbour, Tofino and Bamfield (Rabinovich and Stephenson, 2004). The tsunami of 2 November 2004 was generated by an $M_w = 6.6$ earthquake within the Explorer Plate off Vancouver Island. Tsunami waves associated with this earthquake were recorded at tide gauges at Tofino and Bamfield on the BC coast (Rabinovich, 2005). The apparent efficient generation of tsunamis by these two local earthquakes raises the question of tsunami hazard for this seismically active offshore region. Why these two moderate earthquakes generated tsunami waves and whether the tsunamis were initiated directly by seismic shocks or indirectly by associated landslides is of considerable interest for tsunami research. This paper presents analyses of the tsunami records for the QCI (Section 2) and Explorer Plate

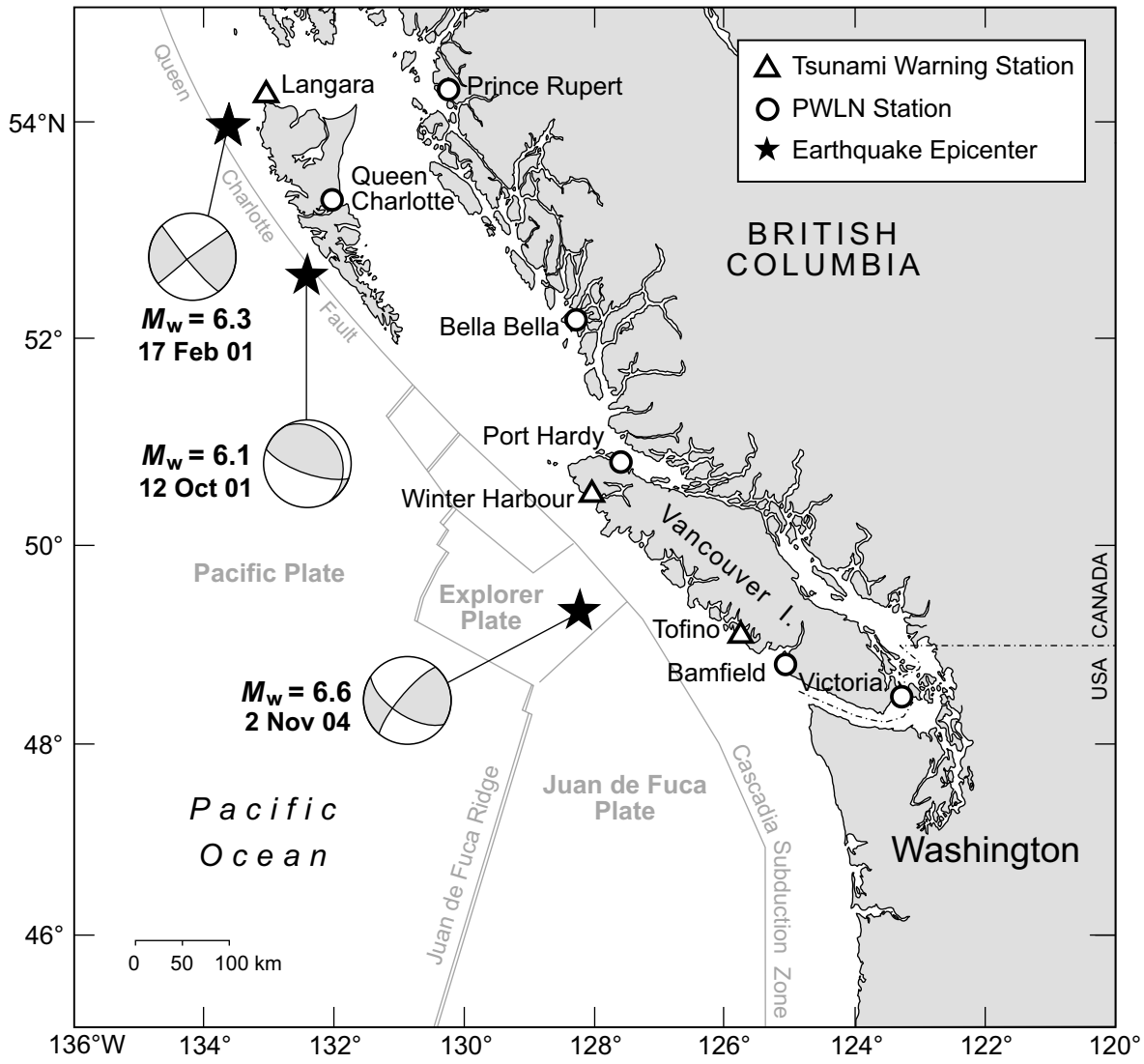

Fig. 1 Epicentres and fault mechanisms for the 12 October 2001 (M_w = 6.1) and 2 November 2004 (M_w = 6.6) tsunamigenic earthquakes. Also shown are the epicentre and fault mechanism for the 17 February 2001 (M_w = 6.3) earthquake for which no tsunami was recorded. Circles denote locations of the Permanent Water Level Network (PWLN) tide gauges and triangles the Tsunami Warning tide gauge sites for the coast of British Columbia. Also shown are the positions of the main plates and faults.

(Section 3) events, with detailed estimates of the statistical and spectral properties of the observed waves along the coast of BC. We also simulate these events numerically and compare the computed and measured waveforms at selected coastal stations. The possibility of destructive tsunamis from local sources other than the CSZ and implications for tsunami hazards for this seismically active region are discussed in Section 4.

2 Queen Charlotte Islands tsunami of 12 October 2001

The 12 October 2001 earthquake had a magnitude M_w = 6.1 and occurred at 05:02 UTC on the continental slope of the QCI at 52°37.56′N, 132°11.70′W (Fig. 1). Shaking was felt all over the QCI and on the adjacent mainland. The earthquake epicentre was located just to the east of the major strike-slip Pacific–North American plate boundary known as the Queen Charlotte Transform Fault (QCF). This fault is seismically very active; the largest instrumentally recorded earthquake in Canadian history, M_w = 8.1 in 1949, was produced by the QCF system (Rogers, 1983). In the southern QCF region of the transform fault, existing compression perpendicular to the fault (Smith et al., 2003) also generated several smaller thrust earthquakes.

A well-constrained moment tensor solution based on regional broadband data from BC and Alaska shows that the 2001 earthquake had almost pure thrust faulting (Fig. 1). Rupture initiated at a depth of about 22 km, typical of many earthquakes in this region, and the centre of energy release as determined by the regional moment tensor solution was about 14 km. This earthquake was the first documented thrust

solution for an event greater than magnitude 6.0 on the predominantly strike-slip plate boundary in this region. There was an extensive aftershock sequence located by the regional seismograph network on the QCI that defined a region about 15 km in diameter.

a *Tsunami Observations and f-t Analysis*

Despite its relatively low magnitude, the October 2001 underwater earthquake generated a tsunami which was clearly recorded by four tide gauges — Bamfield, Tofino, Winter Harbour and Port Hardy (Fig. 2) — on the coast of Vancouver Island (Rabinovich and Stephenson, 2004). Statistical characteristics of the observed waves are presented in Table 1.

Maximum peak-to-trough wave heights for the four gauge sites were quite consistent, ranging from a minimum of 11.3 cm at Bamfield to a maximum of 22.7 cm at Winter Harbour. Unfortunately, the Langara tsunami station was not in operation during this event, while at other PWLN stations, including Queen Charlotte, Bella Bella and Prince Rupert located in the vicinity of the source area (Fig. 1), the tsunami was not recorded apparently because of coastal sheltering. The duration of the most energetic waves ('wave ringing') at Bamfield, Tofino, Winter Harbour and Port Hardy was relatively short, lasting for only 6–8 hours. The 12 October 2001 event appears to have been a local tsunami, originating within coastal BC waters. We note that an earthquake with M_w = 6.3, which occurred on the northwestern coast of the QCI (53°55.31′N, 133°36.78′W) on 17 February 2001 (Fig. 1), did not produce a measurable tsunami probably because it had a strike-slip mechanism.

The expected tsunami arrival times (ETA) for the October 2001 QCI tsunami were estimated for the coasts of BC, Alaska and Washington using the National Oceanic and Atmospheric Administration (NOAA) Method of Splitting Tsunamis (MOST) numerical tsunami model (Titov and Synolakis, 1997; Titov and González, 1997). The calculated ETA (relative to the main shock) is in reasonable agreement with approximate estimates of the observed tsunami travel times for all stations except Port Hardy (Table 1). It is difficult to compare these estimates more precisely. The ability to detect tsunami waves in tide gauge records and to estimate parameters of these waves strongly depends on the signal-to-noise ratio (Rabinovich et al., 2006a). For the two events examined here, background noise at all sites was quite high and the signal-to-noise ratio quite low, especially for Port Hardy. Despite an obvious increase in longwave energy during the event (Fig. 2), the exact arrival time (and the respective travel time) of the first wave was not clearly delineated in the records. At some sites, the tsunami-driven seiches simply augmented the atmospherically generated seiches (eigen oscillations) that were occurring in the corresponding bays, inlets or harbours at the time. Thus, the signs of the first waves presented in Table 1 were not determinable with complete reliability but represent our 'best guess' in each case.

Analyses of the 2004 Sumatra tsunami for the Atlantic and Pacific coasts of North America (Rabinovich et al., 2006a) demonstrated that frequency-time (*f-t*) diagrams could be used effectively to identify tsunami waves and to detect their arrival in noisy records. Thus, to estimate first wave arrival times (Table 1) we used both the de-tided records (Fig. 2) and their corresponding *f-t* diagrams (Fig. 3). To construct these diagrams, we used a method developed by Dziewonski et al. (1969) to study non-stationary seismic signals in which the time series displays rapid temporal changes in amplitude and/or phase. The method, which is similar to wavelet analysis (Emery and Thomson, 2001), is based on narrow-band filters, $H(\omega)$, with a Gaussian window that isolates a specific centre frequency, $\omega_n = 2\pi f_n$:

$$H_n(\omega) = e^{-\alpha\left(\frac{\omega-\omega_n}{\omega}\right)}. \quad (1)$$

The frequency resolution is controlled by the parameter α. The higher the value of α, the better the resolution in the frequency domain, but the poorer the resolution in the time domain (and vice versa.) We used $\alpha = 60$ in our computations. Demodulation of band-passed sea level time series, $\xi(\omega_n;t)$, yields a matrix of amplitudes (phases) of wave motions with columns representing time and rows representing frequency (*f-t* diagrams). This method can be effectively used to identify tsunami waves and to examine how the tsunami wave energy $E(f, t)$ changes as a function of frequency and time (González and Kulikov, 1993; Rabinovich et al., 2006a, 2006b).

Figure 3 presents *f-t* diagrams for tide gauge records on 12 October 2001 at four Vancouver Island stations. The diagrams are constructed for the frequency range 0.007–0.25 cpm (periods 142–4 min). In all four plots, tsunami waves are well-defined and mutually consistent. In particular, the duration of the energetic wave trains following the earthquake are similar (approximately 8 hr). At Winter Harbour, the tsunami energy is mainly concentrated within a wide frequency band corresponding to periods of 25 to 45 min. At Tofino, there are two main energetic frequency bands: (1) at periods 15 to 25 min, and (2) at periods 45 to 60 min. The Port Hardy *f-t* diagram differs slightly from those for Tofino and Winter Harbour in that tsunami oscillations are polychromatic and more chaotic, with typical oscillation periods ranging from 5 to 35 min. At Bamfield, the oscillations have a rather complicated structure with three dominant frequency bands with corresponding peak periods of approximately 60, 30 and 12–18 min.

Analysis of the 2004 Sumatra tsunami for the Pacific coast of North America (Rabinovich et al., 2006a) revealed marked variations in observed wave heights along the coast of North America and significant differences in these heights even for nearby stations. These differences were found to be related to local resonant properties for the individual sites. Rabinovich and Stephenson (2004) examined similar properties for BC sites. In the present study, the energetic frequency bands observed in the *f-t* diagrams (Fig. 3) also coincide with resonant peak frequencies estimated for each particular site.

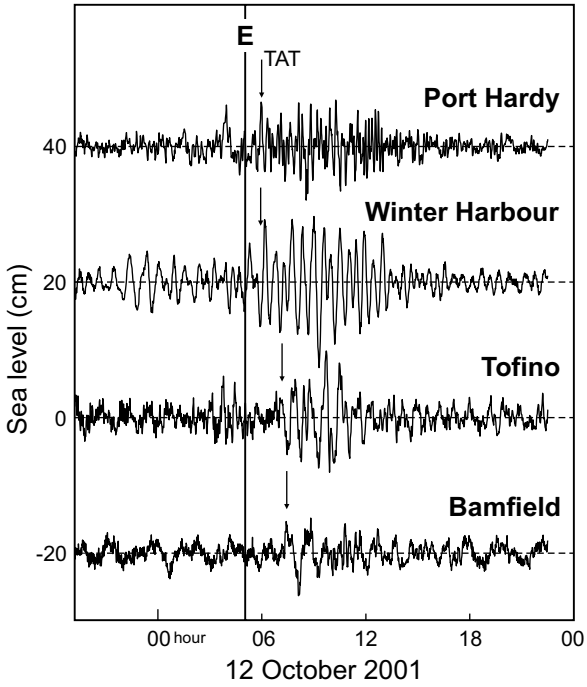

Fig. 2 High-pass filtered records of the 12 October 2001 QCI tsunami at four stations located on the coast of Vancouver Island. The vertical line (E) indicates the time of the main earthquake shock; arrows denote the arrival of the first tsunami wave.

b *Spectral Analysis*

The *f-t* diagrams described in the previous section, as well as similar types of wavelet analysis, are an effective tool for investigating *non-stationary* features of observed tsunami waves (cf. González and Kulikov, 1993; Emery and Thomson, 2001). To examine the overall frequency content of tsunami oscillations formed during the October 2001 QCI event, and to compare this frequency distribution with that of the background oscillations at the same sites, we used spectral analysis. Although not strictly applicable to non-stationary processes, spectral analysis provides insight into the integral characteristics of tsunami signals (cf. Emery and Thomson, 2001). We separated the records (Fig. 2) into two parts. The time span of 25.6 hours preceding the tsunami arrivals was identified as having 'normal' wave conditions and selected for analysis of the background signals. For the 'tsunami' period, we chose the 8.5 hours immediately following the wave arrivals, which are characterized by relatively homogeneous tsunami oscillations (Fig. 2). Our spectral analysis procedure is similar to that described by Emery and Thomson (2001). To improve the spectral estimates, we used a Kaiser-Bessel spectral window with half-window overlaps prior to the Fourier transform. The length of the window was chosen to be 256 min, yielding 6 degrees of freedom per spectral estimate for tsunami spectra and 22 degrees of freedom for background spectra. Figure 4 shows the results of the analysis for all four stations.

In general, the spectra of both tsunami and background are 'red' (analogous to light spectra), with the spectral energy decreasing with increasing frequency as ω^{-2}. This is typical for longwave sea level spectra (cf. Kulikov et al., 1983; Filloux et al., 1991; Rabinovich, 1997). At most stations, differences between tsunami and background spectra occur mainly within the frequency band 0.1×10^{-1} to 2×10^{-1} cpm (periods 100 to 5 min). In this band, the tsunami spectra are approximately 0.5 to 1.0 orders of magnitude higher than in other bands, indicating that the tsunami waves were two to three times higher than the background oscillations being generated predominantly by atmospheric processes. Differences in spectral peaks among the stations (Fig. 4) are indicative of the influence of local topography. The most prominent peaks are observed in tsunami spectra for Winter Harbour (period approximately 30-46 min) and Tofino (approximately 50 min). The frequencies of most peaks in the tsunami spectra at all stations coincide with corresponding peak frequencies in the background spectra. This result is in good agreement with the well-known fact that periods of observed tsunami waves are mainly related to resonant properties of the local/regional topography rather than characteristics of the source, and are almost the same as those of ordinary (background) long waves for the same sites. For this reason, the spectra of tsunamis from different earthquakes are usually similar at the same location (cf. Honda et al., 1908; Loomis, 1966; Miller, 1972; Rabinovich, 1997)[1]. It is therefore difficult to reconstruct the source region spectral characteristics based on data from coastal stations.

TABLE 1. Properties of the 12 October 2001 QCI tsunami estimated from coastal tide gauge records.

			First wave		
Station	Coordinates	Maximum wave height (cm)	(sign) arrival time (UTC)	Travel time	Expected travel time
Bamfield	48° 50′N; 125° 08′W	11.3	(+) 07:20	2 hr 18 min	1 hr 52 min
Tofino	49° 09′N; 125° 55′W	18.2	(+) 07:01	1 hr 59 min	1 hr 44 min
Winter Harbour	50° 31′N; 128° 02′W	22.7	(-) 05:47	0 hr 45 min	0 hr 56 min
Port Hardy	50° 43′N; 127° 29′W	14.5	(+) 05:53	0 hr 51 min	1 hr 38 min

[1] The resonant characteristics of each location are always the same; however, different sources would certainly induce different resonant modes, specifically, low-frequency modes for large seismic sources and high-frequency modes for small seismic sources.

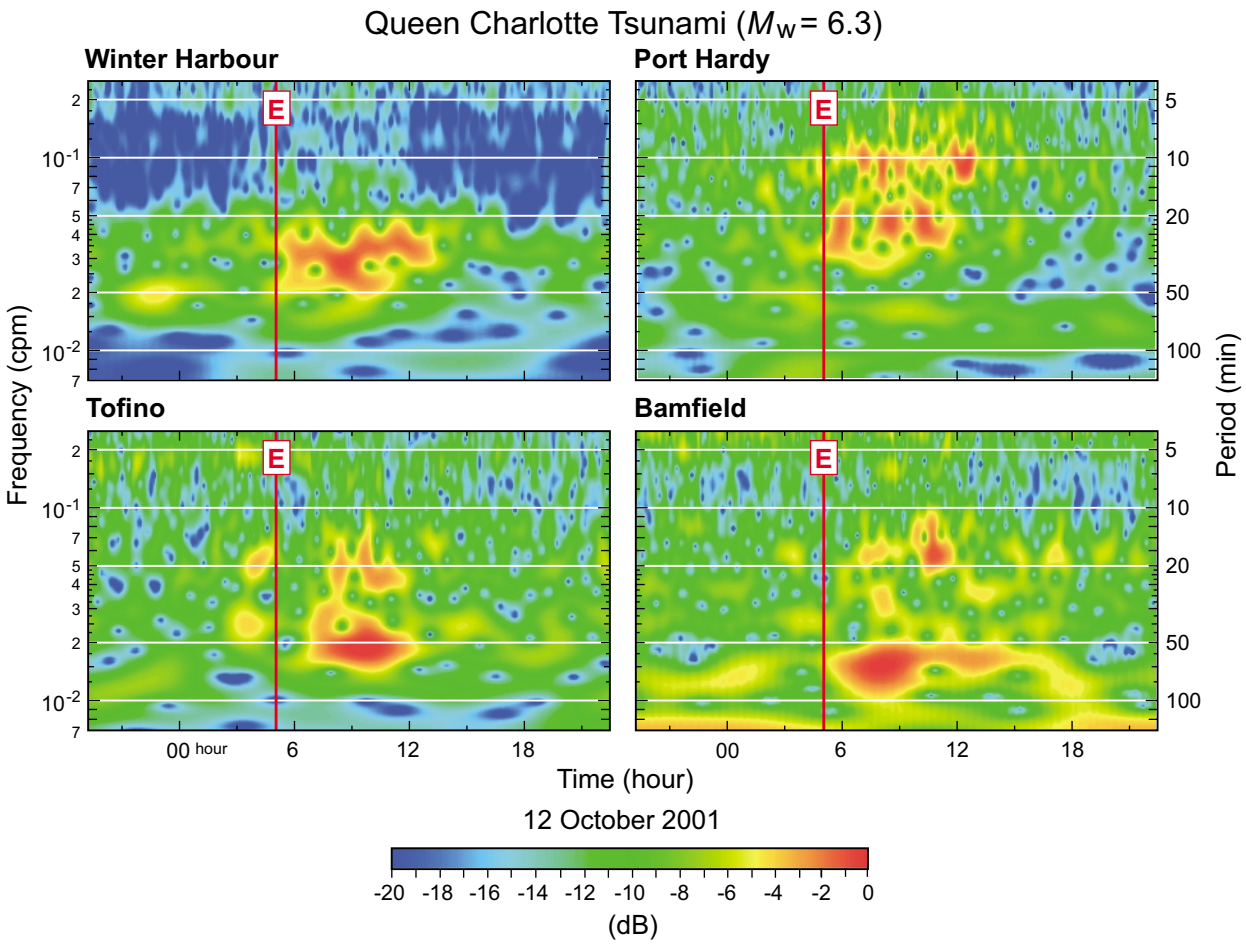

Fig. 3 Frequency-time (*f-t*) diagrams for the 12 October 2001 QCI tsunami for the Winter Harbour, Port Hardy, Tofino and Bamfield tide gauge records. The vertical line (E) indicates the time of the main earthquake shock.

To separate the influences of the local topography and the source, and to reconstruct the open-ocean spectral characteristics of the October 2001 QCI tsunami, we used the method of Rabinovich (1997) (see also Rabinovich and Stephenson, 2004; Rabinovich et al., 2006b). The method is based on the assumption that the spectrum $S(\omega)$ of both tsunami and background sea level oscillations near the coast can be represented as:

$$S(\omega) = W(\omega)E(\omega), \tag{2}$$

where ω is the angular frequency, $W(\omega) = H^2(\omega)$, $H(\omega)$ is the frequency admittance function describing the linear topographic transformation of long waves approaching the coast, and $E(\omega)$ is the source spectrum.[2] Using Eq. (2), we next assume that all individual peculiarities of the observed spectrum $S_j(\omega)$ at the jth site are related to the site-specific topographic function $H_j(\omega)$, while all general properties of this spectrum are associated with the source (assuming that the source is the same for all stations). For typical background oscillations $E(\omega) = S_0(\omega)$, where $S_0(\omega)$ is the longwave spectrum in the open ocean. The function $S_0(\omega)$ is smooth, monotonic and almost universal (cf. Kulikov et al., 1983; Filloux et al., 1991) and roughly described as:

$$S_0(\omega) = A\omega^{-2}, \tag{3}$$

where $A = 10^{-3} - 10^{-4}$ cm^2 cpm is a constant slightly dependent on atmospheric activity and individual properties of the basin. (A tends to be higher in shallow-water basins and during times of high storm activity.)

During tsunami events, sea level oscillations observed near the coast may be presented as:

$$\xi_{obs}(t) = \xi_t(t) + \xi_b(t), \tag{4}$$

where ξ_t are the tsunami waves generated by an underwater seismic source and ξ_b are the background surface oscillations. If the spectra of both tsunami and background oscillations

[2] The 'source spectrum' can be indicative not only of the initial seismic source but also of secondary remote sources associated with open ocean tsunami wave scattering and reflection.

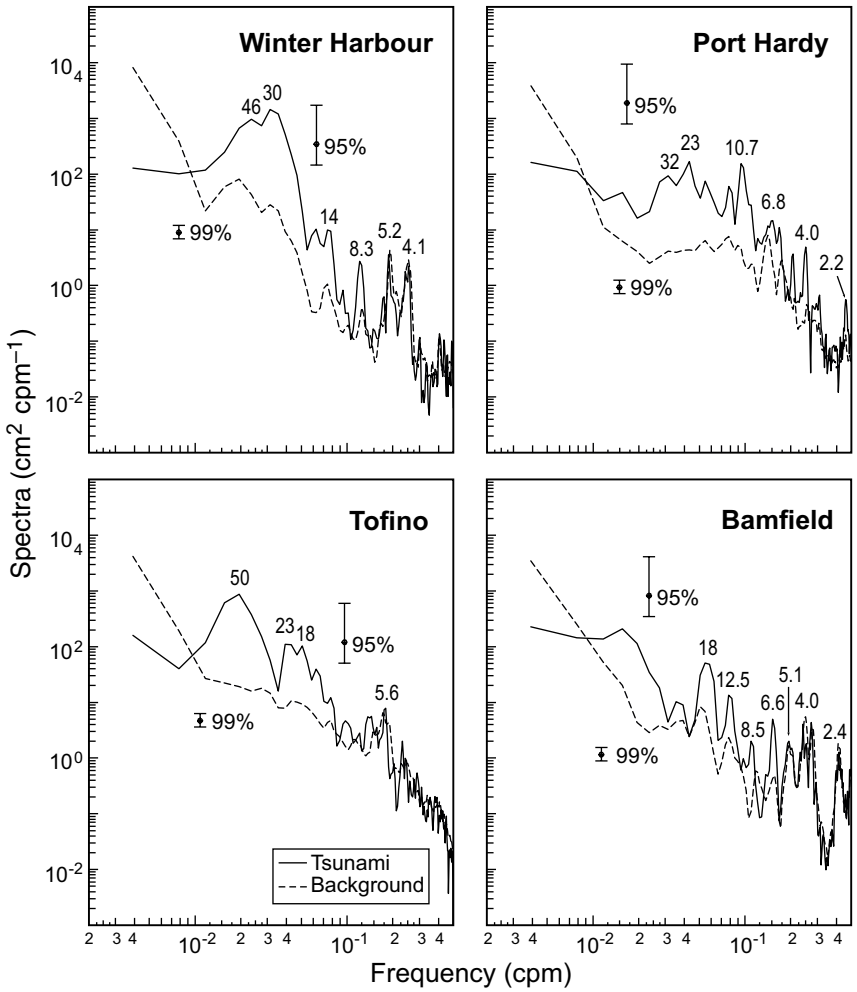

Fig. 4 Spectra of background waves and 12 October 2001 tsunami oscillations for Winter Harbour, Port Hardy, Tofino and Bamfield. Periods (in minutes) of the main spectral peaks are indicated. The 95% confidence level applies to the tsunami spectra, the 99% confidence interval to the background spectra.

have the form of Eq. (2), we can compare these spectra to separate the source and topographic effects. In this way, we assume that the spectra of the observed tsunami and background long waves are a product of the same topographic admittance function, $W(\omega)$. This function is strongly variable in space (due to the resonant properties of local topography) and almost constant in time.[3] Conversely, the corresponding source function is spatially uniform, but varies considerably with time. As demonstrated by Rabinovich (1997), the spectral ratio $R(\omega)$ can be estimated as:

$$R(\omega) = \frac{S_t(\omega) + \hat{S}_b(\omega)}{S_b(\omega)} = \frac{E(\omega) + \hat{S}_0(\omega)}{S_0(\omega)} = A^{-1}\omega^2 E(\omega) + 1.0. \quad (5)$$

where $S_t(\omega)$ is the tsunami spectrum and $\hat{S}_b(\omega)$ and $S_b(\omega)$ are the spectra of background oscillations observed during and before the tsunami event, respectively. This ratio is independent of local topographic influence, is determined solely by the external forcing (i.e., by tsunami waves in the open ocean near the source area) and gives the amplification of the longwave spectrum during the tsunami event relative to the background conditions. Because the ratio has the same characteristics as the external source, it has been termed the 'source function'.[4]

Figure 5 presents individual spectral ratios (source functions) for the QCI tsunami estimated from the four coastal tide gauge stations and the mean function (the average over the spectral ratios for the four stations). To assist with the

[3] In some sense the function W for local longwave oscillations is similar to tidal harmonic constants, which are highly variable in space but constant in time (cf. Pugh, 1987).

[4] The source function defined in the form of Eq. (5) is always *positive,* in contrast to $R(\omega) - 1.0$, which can be negative at frequencies where $S_t(\omega) \sim 0$ and $\hat{S}_b(\omega) < S_b(\omega)$.

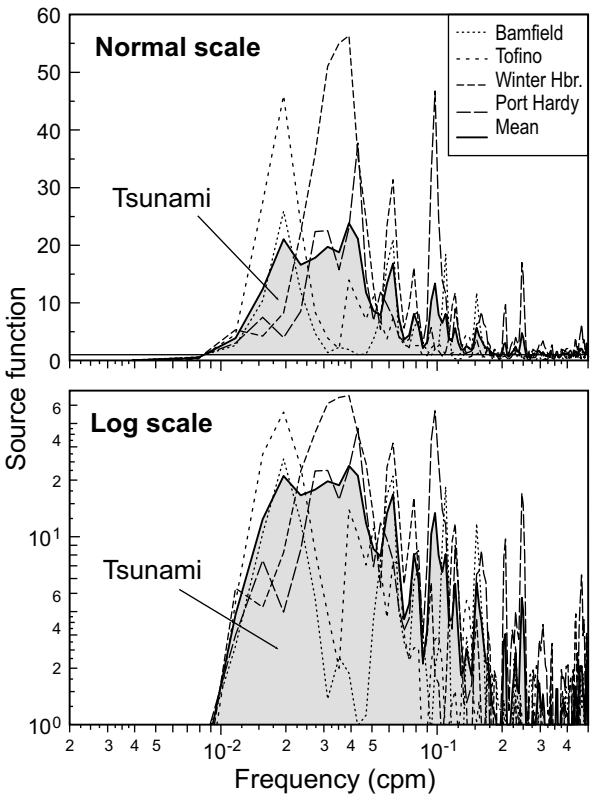

Fig. 5 Source functions of the QCI tsunami of 12 October 2001 reconstructed from the four tide gauge records in Fig. 3 (Bamfield, Tofino, Winter Harbour and Port Hardy) and the corresponding mean source functions for the four sites. Source functions are presented for both linear and logarithmic amplitude scales. The shaded area denotes the tsunami response.

interpretation, the functions are shown with both linear and logarithmic vertical scales. In contrast to the individual spectra (Fig. 4), which show marked differences among sites, the constructed source functions (Fig. 5) have obvious features in common. Evident in the spectral ratio plots is the fact that the tsunami energy is confined to a well-defined frequency band of approximately 0.01–0.25 cpm (periods 100–4 min), with peak values in the range of 0.016–0.12 cpm (62.5–8.3 min). Moreover, this ratio distribution has a more abrupt low-frequency cut-off and gradual decay of the high-frequency 'tail', indicating the presence of a high-frequency component to the tsunami source, an effect that has recently been examined for the 2004 Sumatra tsunami by Hanson et al. (2007) based on hydrophone data. However, the contribution of this high-frequency component to the tsunami wave field is relatively small. Based on the source function, the external forcing (i.e., that forcing associated with the spectral properties of the open-ocean tsunami source) was mainly concentrated at periods from 8–60 min (0.125–0.017 cpm).

c *Numerical Simulation*

We have simulated the 2001 QCI tsunami using the MOST tsunami model (Titov and González, 1997; Titov et al., 2005a, 2005b). Results of the modelling were then compared with the high-quality tide gauge records of the event collected on the BC coast. This model uses a seismically defined seafloor displacement of 1.0 m with dimensions of approximately 30 km × 15 km based on initial regional moment tensor solutions by the Pacific Geoscience Centre (PGC), Geological Survey of Canada (Fig. 1). Due to the spatial location of seismic stations, the PGC source model has a closely determined alongshore (NW–SE) source area position (y) but a less precisely defined cross-shore (SW–NE) location (x). For comparison, we have also used the source models provided by Harvard University and the United States Geological Survey (USGS). Differences in simulated tsunami waves for these three models are not significant.

Global wave propagation was first derived using a coarse, basin-scale numerical grid with roughly 2-minute spatial resolution. The computational domain (Fig. 6a) included the entire northwestern coast of North America from Oregon to southeastern Alaska (45º–60ºN; 140º–122ºW). Solutions for the coarse grid model then drove a nested 250 m fine-grid version of the same model for the coast of Vancouver Island, including the tide gauge sites of Bamfield, Tofino, Winter Harbour and Port Hardy (Fig. 6b). Snapshots of simulated waves (for 0, 30, 60, 90 and 120 min) for the coarse-grid model are shown in Fig. 7. The initial source (Fig. 1) was a dipole with uplift on the southwestern (oceanic) side of the source area and subsidence on the northeastern (continental) side. Consequently, the first positive wave (crest) travelled seaward creating well-defined semi-circular wave crests. In contrast, the first negative wave (trough) travelled landward toward the coast of the QCI (Fig. 7). The first crest reached the northern coast of Vancouver Island about 40 min after the main earthquake shock, consistent with the observations. (The tsunami is first seen as positive waves at Tofino, Bamfield and Port Hardy; Table 1.) However, because of strong shelf/coastline irregularities, the waves were then scattered, leading to trains of irregular trapped waves propagating along the Vancouver Island shelf (Fig. 8). This scattering likely explains why the first tsunami wave at Winter Harbour was negative (Table 1).

Several additional numerical experiments were made for the same source function but for slightly different cross-shore deformation positions (x). Tsunami responses were estimated and modelled wave heights were then compared with the recorded waves at the four tide gauge sites in Fig. 6b. The best agreement between the observed and simulated waves (Fig. 9) was achieved for an earthquake deformation region centred near the toe of the steep continental slope in water depths from 200 to 3000 m. In the case of the observations, the best fit with the model is for Winter Harbour, the gauge site closest to the source and to the open ocean; the poorest fit is for Port Hardy, the gauge site separated from the source area by the most complex and irregular seafloor topography. Computed tsunami amplitudes at Port Hardy are only about 1.5 cm, while ordinary seiches commonly observed at this site (likely associated with atmospheric activity) are 4 to 5 times

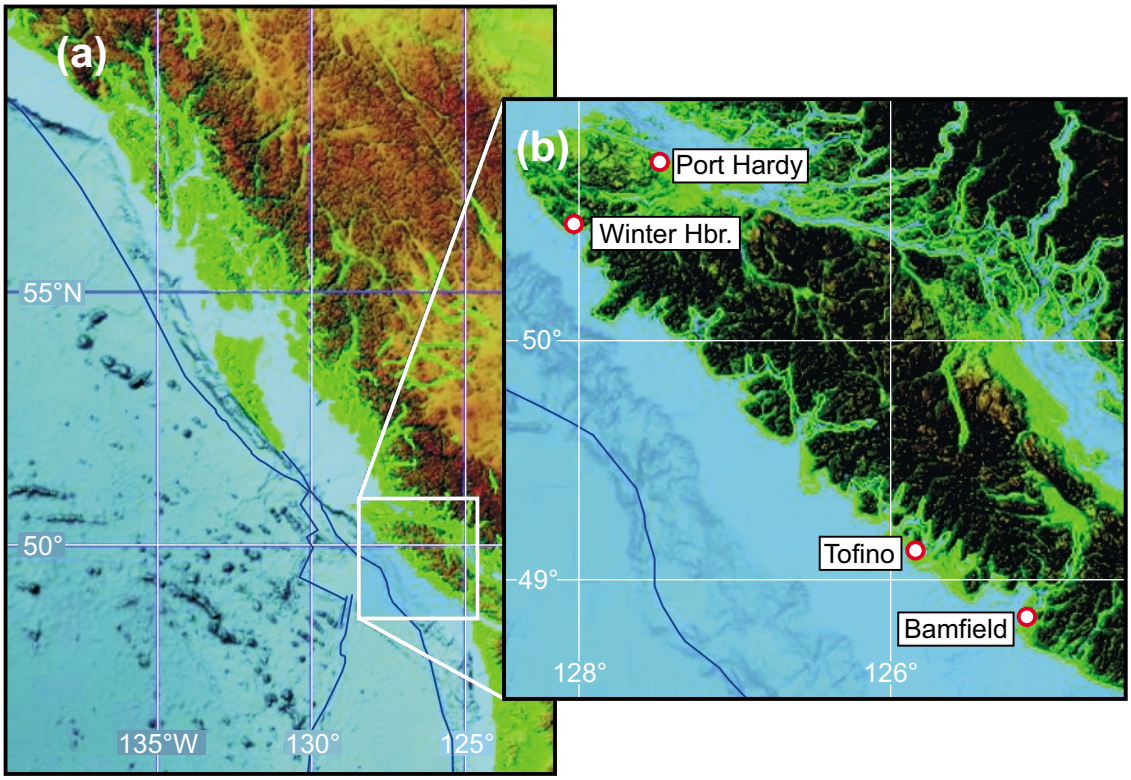

Fig. 6 Computational domains used for numerical simulation of the 2001 QCI tsunami: (a) the coarse (2′ or approximately 3.7 km) resolution domain, and (b) the fine (250 m) resolution domain for the Vancouver Island region. Tide gauge sites are shown in (b).

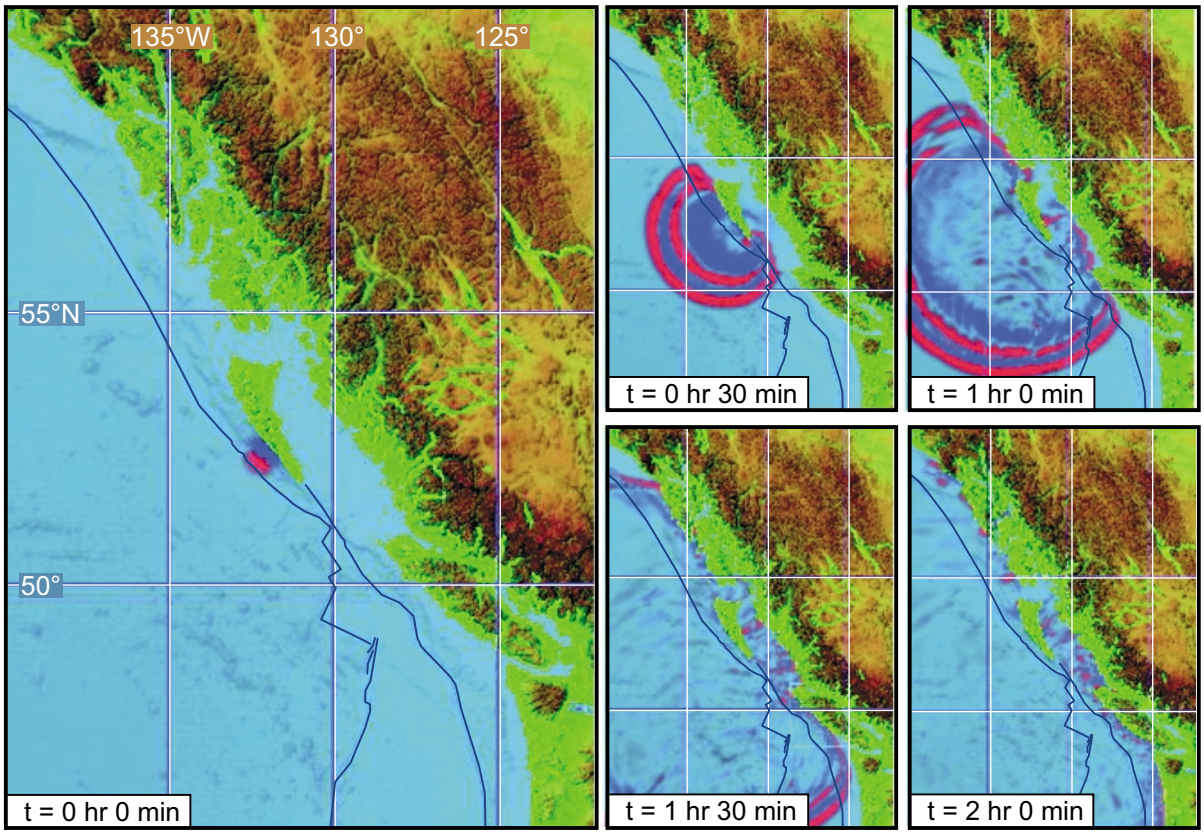

Fig. 7 Snapshots of the numerically simulated tsunami wave crests for the 2001 QCI tsunami for the coarse-grid model at times 0, 30, 60, 90 and 120 min after the main earthquake shock.

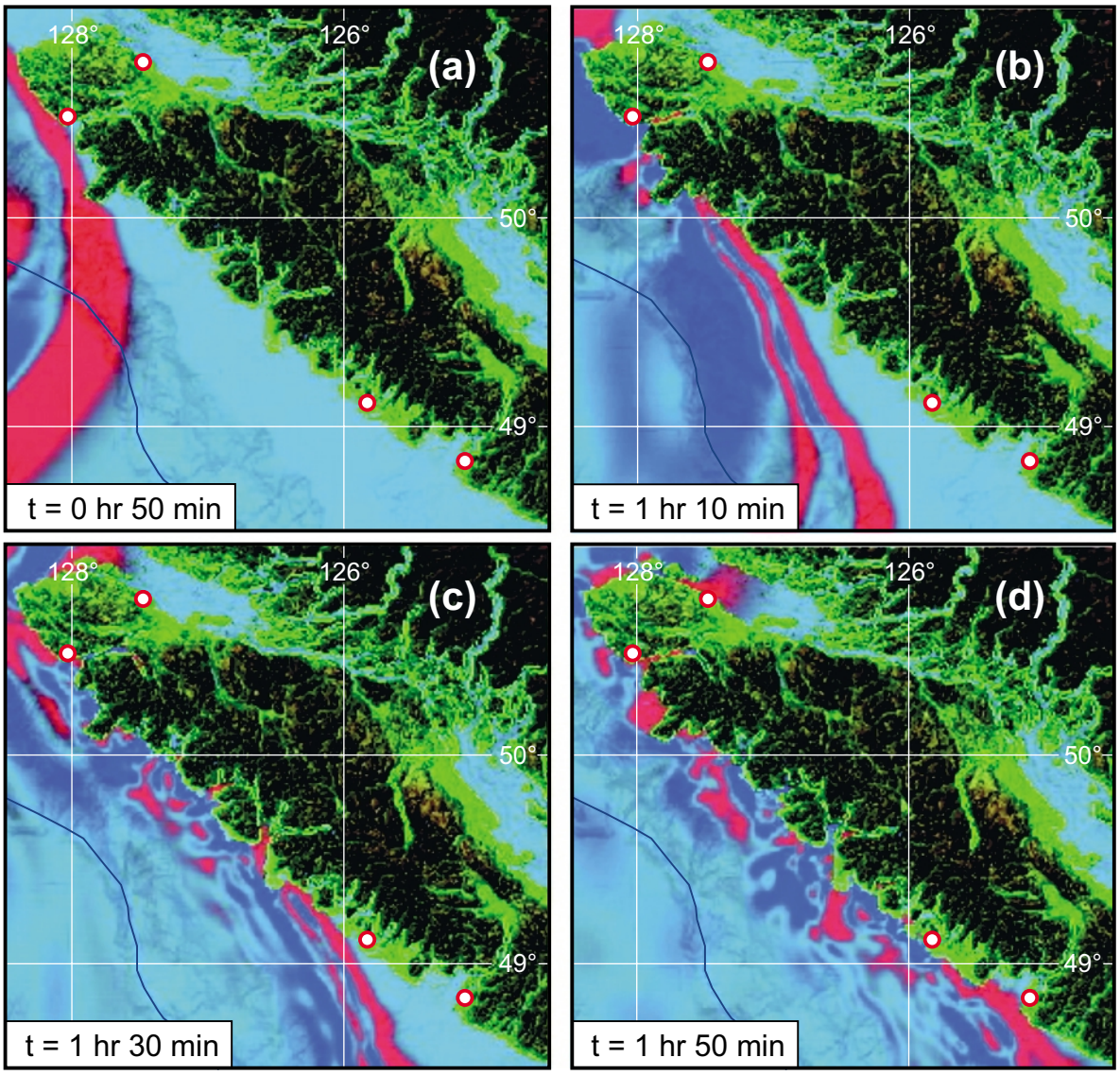

Fig. 8 As in Fig. 7 but for the vicinity of Vancouver Island for times 50, 70, 90 and 110 min after the main earthquake shock.

larger, making close wave simulation almost impossible. Tsunami predictions for Tofino and Bamfield are further affected by the lack of high resolution bathymetric data and by the local resonance response characteristics of Clayoquot Sound and Barkley Sound, unresolved in the model. Despite these problems (which are typical for modelling weak tsunamis in coastal areas), the simulated wave heights are consistent with observations.

3 Explorer Plate Earthquake and Vancouver Island Tsunami of 2 November 2004

West of Vancouver Island, two small tectonic plates — the Juan de Fuca and Explorer plates — are being subducted beneath the North American continent. An intense swarm of earthquakes occurred within the Explorer Plate about 200 km west of Vancouver Island during the first week of November 2004. More than 700 earthquakes were detected. While swarm activity is not uncommon in the tectonically active, thin oceanic lithosphere west of Vancouver Island, this swarm was unusual because it did not occur along any of the previously recognized offshore fault zones. The largest event (M_w = 6.6) occurred on 2 November at 10:02 UTC. The earthquake epicentre (49° 0.72′N, 129° 10.86′W) was located about 190 km from Port Hardy and 230 km from Tofino. The earthquake generated was felt mildly on northern Vancouver Island, but there were no reports of damage. Locations and focal mechanisms from regional moment tensor solutions of the larger earthquakes reveal a previously unknown left-lateral strike-slip fault about 80 km long within the Explorer Plate (Fig. 10). It trends about 15 degrees counter-clockwise to the very active Nootka Fault Zone. Rupture length of the largest earthquake (M_w = 6.6) in the sequence swarm was about 40 km, estimated from the empirical Green's function

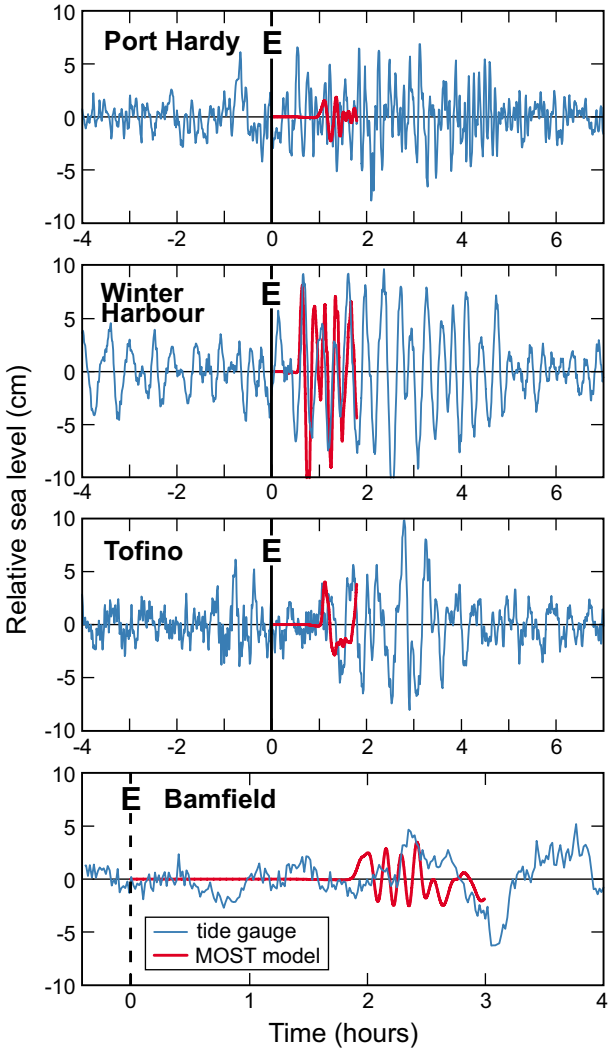

Fig. 9 MOST simulated (short duration thick red line) and observed (full duration thin blue line) tsunami records for Winter Harbour, Port Hardy, Tofino and Bamfield (Vancouver Island) for the 2001 QCI tsunami.

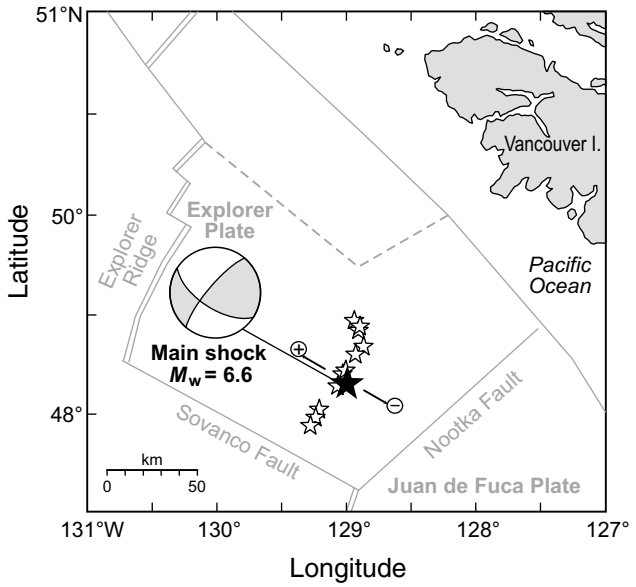

Fig. 10 The larger earthquakes of the swarm (empty stars) that occurred in November 2004 offshore from Vancouver Island. The epicentre of the main shock (M_w = 6.6) is indicated by a filled star and the respective fault mechanism is shown. Also shown are the positions of the main faults. The plus and minus signs indicate the polarity of the generated tsunami wave.

technique using surface waves. While most of the motion was strike-slip, there was a small thrust component with the east side down (Fig. 10).

a *Tsunami Observations*

Examination of the digital records for nearby tide gauge stations (Winter Harbour, Port Hardy, Tofino, Bamfield and Victoria; Fig. 1) reveals that the November 2004 earthquake generated a weak tsunami, which was measured at Tofino and Bamfield only on the outer southwest coast of Vancouver Island (Fig. 11). The maximum recorded trough-to-crest wave heights (Table 2) of 10.8 cm at Tofino and 7.5 cm at Bamfield, are approximately 35% smaller than for the October 2001 QCI tsunami (Table 1). This suggests that the November 2004 earthquake was a markedly less efficient source mechanism.

As noted earlier, our ability to detect tsunami waves in a tide gauge record and to identify the exact arrival time is highly dependent on the signal-to-noise ratio of the data. For the November 2004 tsunami, this ratio was approximately 1.5:1, making this event difficult to detect. In contrast, the ratio for the 2001 tsunami (at least for Tofino and Winter Harbour) was approximately 3:1 (Fig. 2). As with the 2001 QCI tsunami, we had difficulty determining the exact arrival time (and the respective travel time) of the first tsunami wave. In this regard, use of *f-t* diagrams (Fig. 12) again proved helpful. The observed tsunami travel times of 52 and 75 min for Tofino and Bamfield, respectively, were in reasonable agreement with the expected tsunami travel time of 58 min and 70 min (Table 2). The first tsunami semiwave recorded on the coast was negative (wave trough) agreeing with the southeast slide-down motion of the fault (Fig. 10). This caused a negative wave to travel outward to the southeast and a positive wave to move outward to the northwest (Fig. 10).

Formulation of the *f-t* diagrams for the 2004 Vancouver Island tsunami follows that for the 2001 QCI tsunami. The main difference between the two tsunamis is that the energy of the 2004 tsunami at Tofino and Bamfield was mainly concentrated at high frequencies (at periods less than 30 min). Consequently, the *f-t* diagrams (Fig. 12) are focused in the frequency band 0.033–0.5 cpm (periods 30–2 min). For both stations, the *f-t* diagrams reveal well-defined tsunami waves and arrival times. At Tofino, the main energy band was 0.14–0.20 cpm (periods 7–5 min). An increase in energy is also seen at periods 15 to 25 min. At Bamfield there are two frequency bands of high energy and both are at relatively high frequencies of 0.2–0.3 cpm (period 5–3 min) and

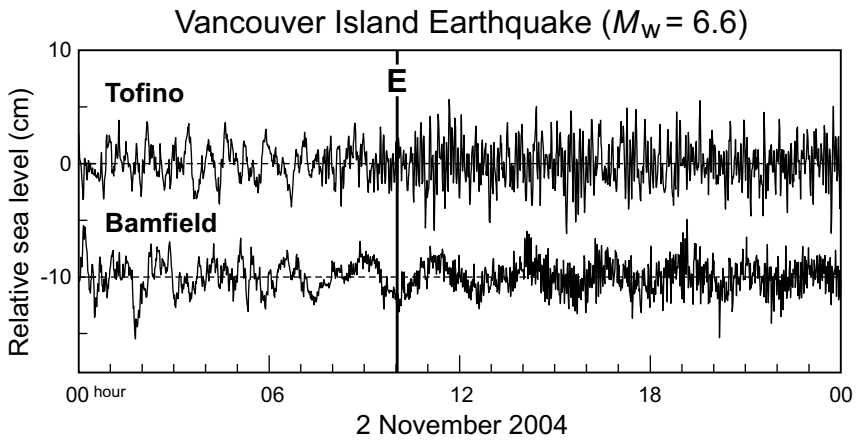

Fig. 11 High-pass filtered records of the 2 November 2004 Vancouver Island tsunami at Bamfield and Tofino, Vancouver Island. The vertical line (E) indicates the time of the main, M_w = 6.6, earthquake shock.

TABLE 2. Statistical properties of the 2 November 2004 Vancouver Island tsunami as estimated from coastal tide gauge records.

			First wave		
Station	Coordinates	Maximum wave height (cm)	(sign) arrival time (UTC)	Travel time	Expected travel time
Tofino	49° 09′N; 125° 55′W	10.8	(-) 10:54	0 hr 52 min	0 hr 58 min
Bamfield	48° 50′N; 125° 08′W	7.5	(-) 11:15	0 hr 75 min	0 hr 70 min

0.4–0.5 cpm (periods 2.5–2 min). For both Tofino and Bamfield, tsunami oscillations for the 2004 Vancouver Island tsunami were of much higher frequency than for the 2001 QCI tsunami. The durations of the tsunami signals also differed. Although the 2004 tsunami (as recorded at coastal stations) was weaker than the 2001 tsunami, the duration of the energetic wave trains ('ringing') observed at Tofino and Bamfield was much longer for the 2004 event: more than 18 hours compared to 8 hours for the 2001 event (cf. Figs 12 and 3).

b *Spectral Analysis*

Estimation of the spectral properties for the November 2004 records at Tofino and Bamfield follows that for the October 2001 tsunami. The only difference is in the lengths of the time segments that we analyzed. The 'ringing' of the 2004 event lasted longer, hence for the analysis of 'tsunami' periods following the wave arrivals, we chose a longer time length of 12.8 hours (compared to 8.6 hours for the 2001 event). Also the signal-to-background ratio for the 2004 tsunami was small (1.5:1). Therefore, to reduce the effect of random processes during analysis of the background noise, we selected a comparatively long time period of 4.5 days preceding the tsunami arrivals. The length of the chosen Kaiser Bessel window was 256 min, yielding 10 degrees of freedom per spectral estimate for tsunami spectra and 98 degrees of freedom for background spectra. Spectral results are shown in Fig. 13.

Spectra for the October 2001 and November 2004 events are similar. Both display 'red' spectral distributions in which energy decreases with increasing frequency as ω^{-2} (compare Figs 4 and 13). At Bamfield, spectra in the band from 2.4 to 18 min have almost identical peak periods at 2.4, 3.5, 4.0, 5.1, 8.5, 12.5–13 and 18 min. The spectral peak at 5.6 min at Tofino is the same for the two events, while two other peaks differ only slightly: 16 and 21 min for the 2001 tsunami (Fig. 4) and 18 and 23 min for the 2004 tsunami (Fig. 13). The primary difference is that only for the 2001 event were there peaks at low frequencies (periods approximately 50–60 min) in the Tofino and Bamfield spectra. We also note that the difference between tsunami and background spectra for the 2004 event is much smaller than for the 2001 tsunami, indicating that the 2004 tsunami was weaker and that the recorded tsunami waves were only a little higher than the background oscillations.

The source function, $R(\omega)$, for the 2004 tsunami (Fig. 14) shows amplification of the longwave tsunami spectrum, relative to background, occurred in the frequency band 0.04–0.5 cpm (periods 25–2 min) with peak values at 0.08–0.25 cpm (periods 12.5–4 min). This is significantly different from what was observed for the 2001 QCI tsunami (Fig. 5) where the main tsunami energy was in the frequency range 0.016–0.12 cpm (periods 60–8 min). These frequency differences are likely associated with differences in the seismic source parameters, in particular with source extensions and ocean depths in the generation areas. Also, the source

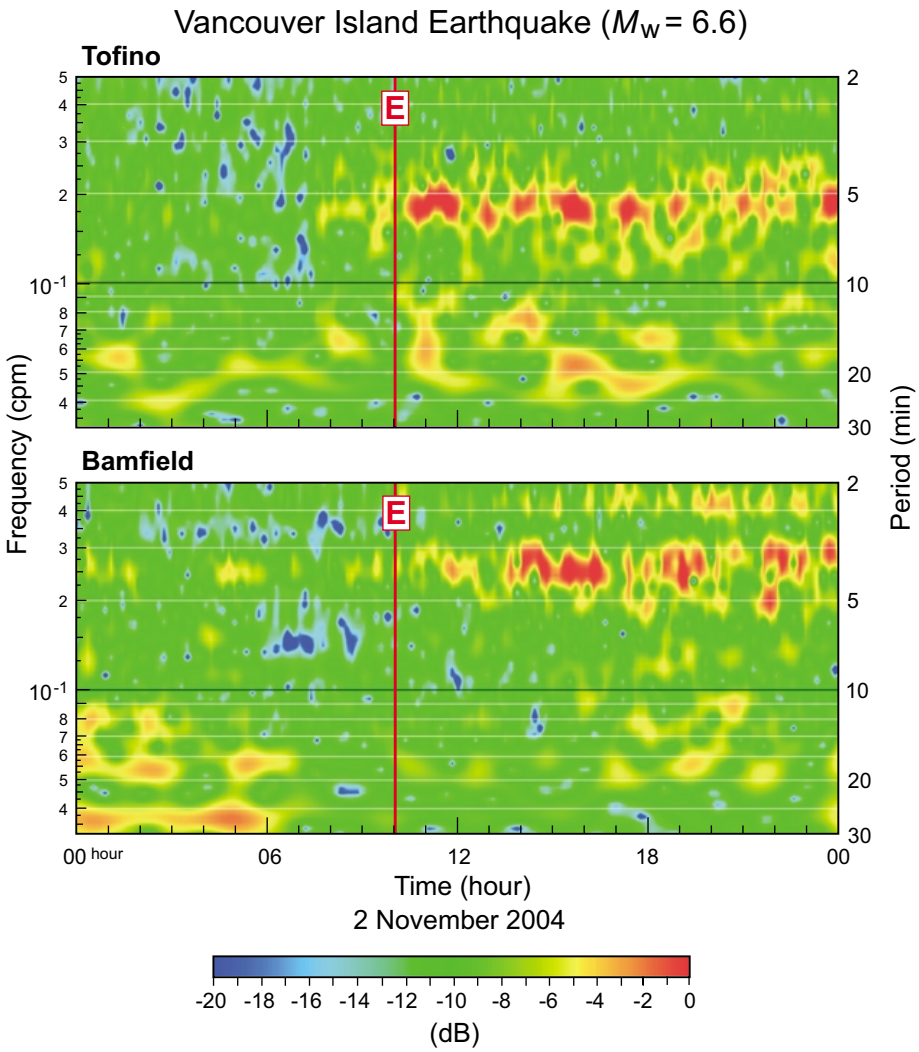

Fig. 12 Frequency-time (*f-t*) diagrams for the 2 November 2004 Vancouver Island tsunami for the Bamfield and Tofino tide gauge records. The vertical line (E) indicates the time of the main earthquake shock.

function values for the 2004 event were approximately three to four times smaller than for the 2001 event, indicating that the 2004 tsunami was significantly weaker than the 2001 tsunami, despite the fact that the magnitude of the 2004 earthquake was considerably larger.

c *Numerical Simulation*

Recorded amplitudes for the 2 November 2004 Vancouver Island tsunami were only slightly above the background signal (Fig. 11) and much smaller than those for the 2001 QCI tsunami (Fig. 2). The observed 2004 tsunami also had notably higher frequencies (compare Figs 5 and 11). Simulations to reproduce such observations present formidable challenges that require high resolution numerical models with quality, high resolution bathymetric data. Consequently, to examine this event and to compare resulting tsunami characteristics with those of the 2001 tsunami, we once again used the MOST tsunami model (Titov and González, 1997; Titov et al., 2005a, 2005b) to simulate the tsunami generation and propagation.

The earthquake parameters used to simulate the 2004 tsunami are based on the USGS Fast moment tensor solution with M_w = 6.6, a strike angle of 222°, a dip angle of 86°, and a slip angle of 8°. Fault sizes used in the simulation were 80 km (length) and 40 km (width) with a slip of 20 cm and epicentre at 49° 0.72′N, 129° 10.86′W. Figure 15 shows the initial sea surface displacement and snapshots of the tsunami propagation for 30, 60, 90 and 120 min. The sea surface deformation pattern for the 2004 tsunami is visibly different from that for the 2001 tsunami source. The strike-slip mechanism of the 2004 earthquake creates a typical asymmetric pattern for the bottom deformation, with substantially smaller vertical amplitudes and shorter waves when compared with the results of the thrust fault model of the 2001 earthquake. Consequently, the resulting 2004 tsunami wave front has an asymmetric shape and smaller amplitudes.

Figure 16 shows the maximum simulated offshore tsunami amplitudes for the 2 November 2004 Vancouver Island earthquake. The cross-shore orientation of the source area creates

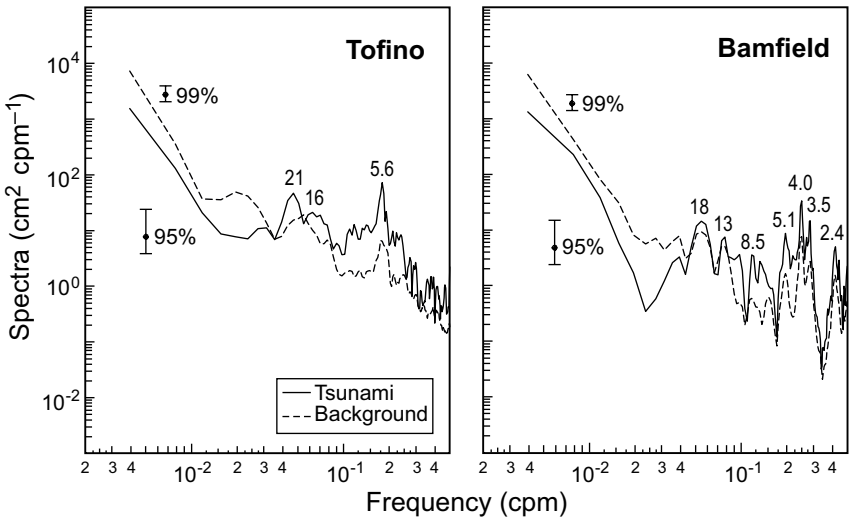

Fig. 13 Spectra of background waves and the 2 November 2004 tsunami oscillations for Bamfield and Tofino. Periods (minutes) of the main spectral peaks are indicated. The 95% confidence level applies to the tsunami spectra and the 99% interval to the background spectra.

the specific cross-shore structure of the simulated wave amplitudes. The maximum computed amplitudes, which are not more than 3 cm offshore, would result in a signal at coastal tide gauges of only a few centimetres. The resolution of the model does not allow for simulation of the near-shore dynamics of these relatively short waves. Nevertheless, offshore features of the model are consistent with the observation of very small amplitude, short-period waves at Tofino and Bamfield for the November 2004 event.

4 Discussion and conclusions

This study presents a detailed analysis of the first instrumental measurements of tsunamis generated by two moderate earthquakes located near the coast of BC. Although the 12 October 2001 QCI and 2 November 2004 Vancouver Island tsunamis were relatively minor events, the very fact that they occurred in this region is of considerable scientific interest and practical importance. The earthquakes were not associated with the CSZ, which is considered to be the main threat for a catastrophic earthquake and tsunami for the coasts of BC and the northwestern United States, but rather with faults located offshore from Vancouver Island and the QCI. The generation of these tsunamis supports the suggestion by Rapatz and Murty (1987) and Murty (1992) of a potential risk to the coast of BC from major tsunamis associated with local non-Cascadian earthquakes.

A key question is why such moderate earthquakes (M_w = 6.1 and 6.6) produced tsunamis in this region. The tsunami from the October 2001 M_w = 6.1 QCI earthquake, which generated waves at four sites with heights ranging from 11 to 23 cm, is particularly intriguing. This earthquake has some of the characteristics typical of a 'tsunami earthquake' (cf. Kanamori, 1972; Abe, 1979) because the effective seismic source — which has a length scale of about 30 km based on comparisons of our tsunami model with tide gauge observations — is considerably larger than the actual seismic source of approximately 15 km expected from the magnitude and aftershock distributions of the generating earthquake. It is likely that the rupture extended into the soft sediments of the

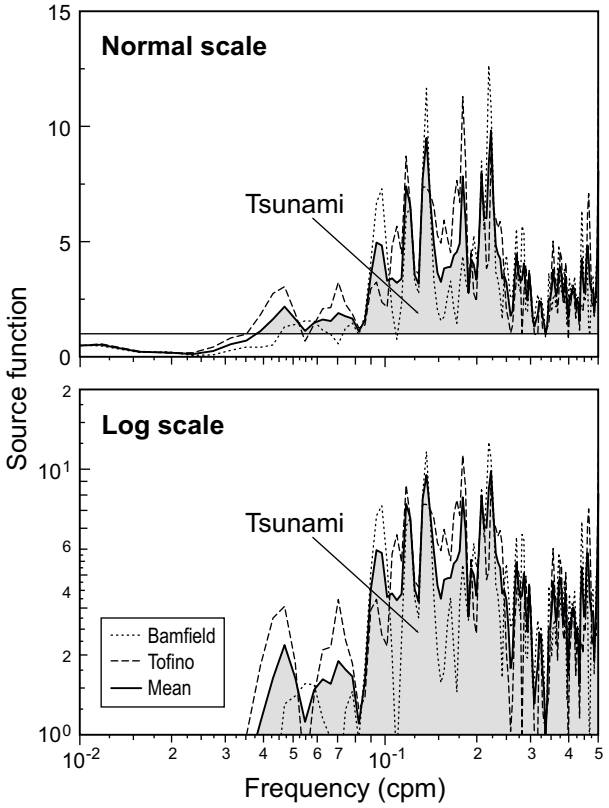

Fig. 14 Source functions for the 2 November 2004 Vancouver Island tsunami reconstructed from the tide gauge records at Bamfield and Tofino (Fig. 13). Source functions are presented for both linear and logarithmic amplitude scales. The shaded area denotes the tsunami response.

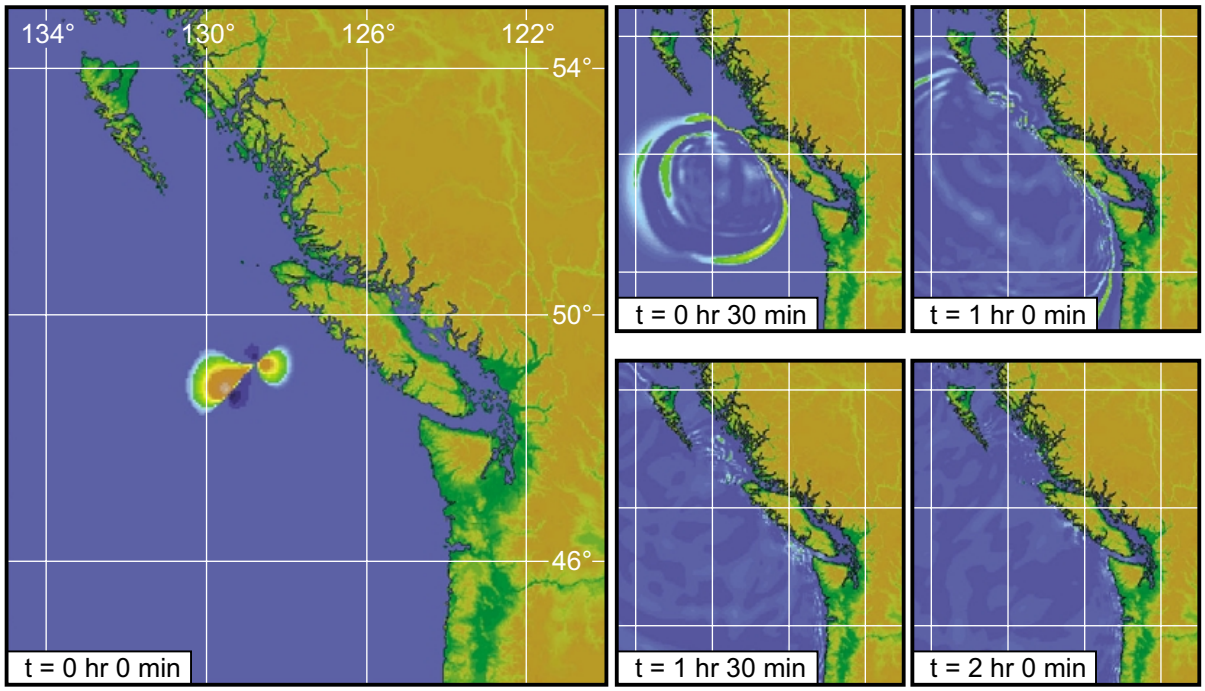

Fig. 15 Snapshots of the numerically simulated wave crests for the 2004 Vancouver Island tsunami at 0, 30, 60, 90 and 120 min after the main earthquake shock.

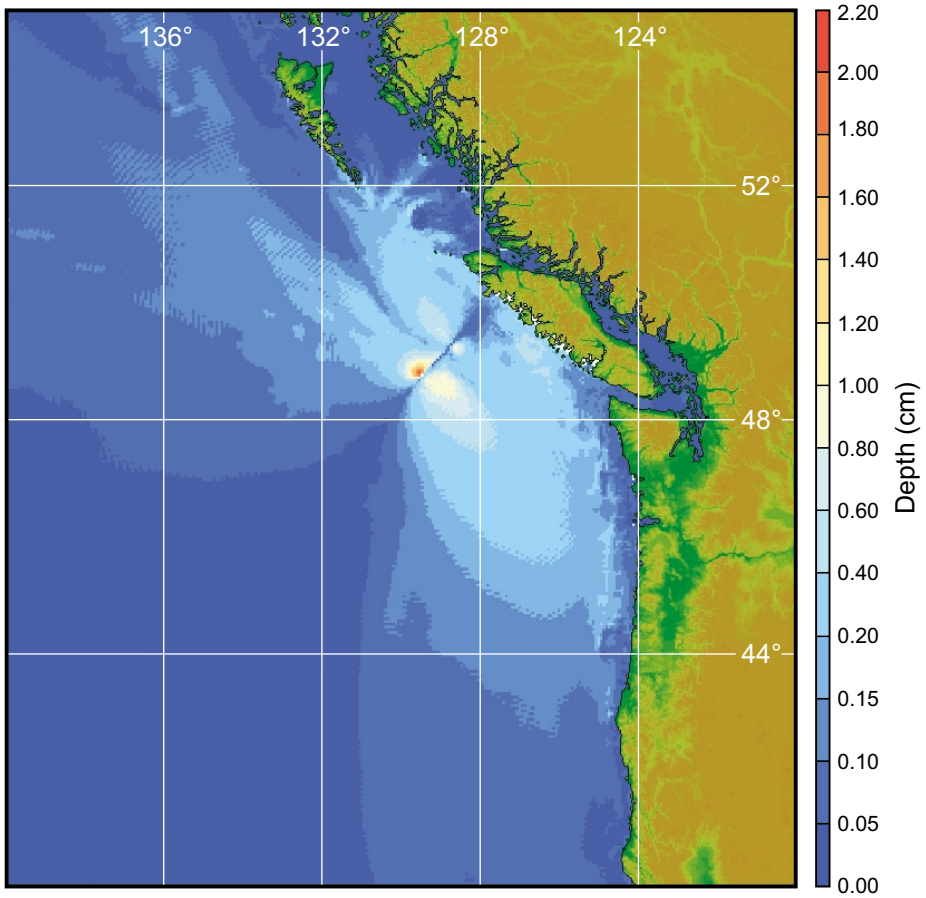

Fig. 16 Maximum amplitudes for the numerically simulated 2004 Vancouver Island tsunami.

Queen Charlotte terrace, thus exceeding the effective displacement for a typical earthquake of this size. This effect was first proposed by Okal (1988) and has more recently been investigated by Geist and Bilek (2001). Okal (1988) suggested that an event for which 10% of the earthquake moment release takes place in sediments can generate a tsunami that is 10 times larger than its seismic moment would indicate. The Queen Charlotte terrace is analogous to the sedimentary accretionary prism found in most subduction zones, capped with up to 2 km more of flat-lying softer sediments.

The QCI have a history of large earthquakes but most of them have strike-slip mechanisms. The Great QCI earthquake (M_w = 8.1) of 22 August 1949 was predominantly strike-slip motion (Rogers, 1986) and produced only a minor tsunami recorded in southeastern Alaska and the Hawaiian Islands (Soloviev and Go, 1975). It has been recently recognized that even though this is predominantly a strike-slip plate boundary, tsunamigenic earthquakes might be possible in the compressive part of the tectonic regime off the southern QCI (e.g., Smith et al., 2003). This is the first documented tsunami to come from that southern region.

Another possibility for the larger-than-expected tsunami in 2001 is that the earthquake triggered a local submarine landslide, which was then the source for the recorded tsunami. Such an event occurred near the coast of Papua New Guinea on 17 July 1998, when an M_w = 7.1 earthquake triggered a submarine landslide that generated a locally catastrophic tsunami which killed more than 2200 people (cf. Synolakis et al., 2002). Caplan-Auerbach et al. (2001) show that large underwater landslides have recognizable acoustical signatures. However, this particular event did not have such a signature on the US Navy SOund SUrveillance System (SOSUS) hydrophone array (R. Dziak, personal communication, 2002). Moreover, there is reasonable agreement between the numerically simulated tsunami (based on the seismic source parameters) and the observed tsunami records (Fig. 9) implying that it was the seismic event that triggered the tsunami.

The Okal (1988) model can also explain why the waves associated with the 2001 QCI earthquake were of relatively low frequency. Tsunami waves generated near the source area would have had typical periods $T \sim 2L/c$, where L is the extension of the source, $c = \sqrt{gh}$ is the longwave speed, g is the acceleration due to gravity and h is the water depth in the source region. For $h \sim 1000$ m, $c \sim 100$ m s^{-1}, and $L \sim 15$ km (from seismic estimates), we find $T \sim 5$ min, which is a factor of 6 to 8 less than the typical observed wave periods of roughly 30–40 min for the 2001 tsunami (Fig. 5). This contradiction can only be resolved if we assume that the actual tsunami source included a portion of the (shallow) continental shelf and was considerably larger, because of the contribution from the slope sediments as per the Okal (1988) model. For the 2004 Vancouver Island tsunami, $h \sim 2500$ m and $c \sim 160$ m s^{-1}. According to seismic data, the rupture length was $L \sim 40$ km. We therefore obtain, $T = 2L/c \sim 8$ min which is in good agreement with the observed tsunami periods (Fig. 14). Thus, in this case, the source region estimated from the fundamental period of the observed waves agrees well with the size estimate for the seismic source area.

In summary, the basic differences between the 2001 and 2004 tsunamis are as follows:

(1) Although the 2001 earthquake (M_w = 6.1) was weaker than the 2004 earthquake (M_w = 6.6), the sea level response was markedly stronger for the 2001 event. Maximum recorded wave heights were 22.7 cm and 10.8 cm, respectively. Also, typical source function values (tsunami versus background noise energies) were $R(\omega) \cong 20$ for the 2001 tsunami and $R(\omega) \cong 4$–6 for the 2004 tsunami.
(2) Typical periods of the 2001 tsunami were significantly longer than for the 2004 tsunami: 8–60 min versus 4–12.5 min.
(3) The 2001 tsunami was characterized by relatively short duration ringing of about 8 hours while the 2004 tsunami had a relatively long ringing duration of more than 18 hours.
(4) The first waves recorded at three of the four Vancouver Island tide gauges for the 2001 tsunami were *positive*, while the first waves recorded at Tofino and Bamfield during the 2004 event (the only sites recording these waves) were *negative*.

Our results demonstrate that the observed differences in the tsunami wave parameters are due to major differences in their respective seismic sources: pure thrust faulting for the 2001 earthquake versus strike-slip faulting for the 2004 event (Fig. 1). The orientations of the main ruptures for these two events were also different, being parallel to the shore for the 2001 earthquake and almost perpendicular to the shore for the 2004 earthquake. The efficient generation of these two BC tsunamis by moderate earthquakes in this seismically active offshore region also points to high potential tsunami risk for the coast of BC that may originate from source areas other than the CSZ.

Contrary to accepted understanding, our findings demonstrate that local earthquakes with magnitudes far below the generally accepted threshold level of 7.0 are capable of generating significant tsunamis. This derives from the fact that modern instrumentation and analysis methods are now capable of detecting such waves within noisy tide gauge records. More specifically, our successful recording and identification of two weak local tsunamis is a direct consequence of modernization of the existing tide gauge network for the coast of BC undertaken by the Canadian Hydrographic Service in 1998. Findings demonstrate that similar events probably occurred in this region many times in the past (e.g., during the period 1905–80 considered by Wigen (1983)) but could not be recorded or detected because of inadequate instrument resolution and recording.

Acknowledgements

We gratefully acknowledge Isaac Fine and Josef Cherniawsky, Institute of Ocean Sciences (Sidney, BC) for

their advice and help with the tsunami travel time computations and John Ristau of the Pacific Geoscience Centre (Sidney, BC) who calculated the regional moment tensor solutions. We also thank Denny Sinnott and Neil Sutherland of the Canadian Hydrographic Service (Sidney, BC) for their assistance in assembling and verifying the tide gauge data, Maxim Krassovski, University of Victoria, for helping with the map plots, and Patricia Kimber of Tango Design (Sidney, BC) for drafting the figures. The authors would like to thank Zygmunt Kowalik of the University of Alaska (Fairbanks) and one anonymous reviewer for their interesting and useful comments. Partial financial support for A.B. Rabinovich was provided by the Russian Federation through RFBR Grants 05-05-64585 and 06-05-08108. This is contribution no. 20070611 of the Geological Survey of Canada (ESS-GSC).

References

ABE, K. 1979. Size of great earthquakes of 1837–1974 inferred from tsunami data. *J. Geophys. Res.* **84**: 1561–1568.

ADAMS, J. 1990. Paleoseismicity of the Cascadia subduction zone: Evidence from turbidites off the Oregon-Washington margin. *Tectonics,* **9**: 569–583.

ATWATER, B.F.; S. MUSUMI-ROKKAKU, K.SATAKE, Y. TSUJI, K. UEDA and D.K. YAMAGUCHI. 2005. *The Orphan Tsunami of 1700*. U.S. Geological Survey, UW Press, Seattle, WA.

CAPLAN-AUERBACH, J.; C.G. FOX and F.K. DUNNEBIER. 2001. Hydroacoustic detection of submarine landslides on Kilauea volcano. *Geophys. Res. Lett*. **28**: 1811–1813.

CHERNIAWSKY, J.Y.; V.V. TITOV, K. WANG and J.-Y. LI. 2007. Numerical simulations of tsunami waves and currents for southern Vancouver Island from a Cascadia megathrust earthquake. *Pure Appl. Geophys.* **164** (2/3): 465–492.

CLAGUE, J.J. 2001. Tsunamis. *In*: A Synthesis of Geological Hazards in Canada. G.R. Brooks (Ed.), Geol. Surv. Canada, Bull. 548, pp. 27–42.

CLAGUE, J.J. and P.T. BOBROWSKY. 1999. The geological signature of great earthquakes off Canada's west coast. *Geosci.* **26** (1): 1–15.

CLAGUE, J.J.; A. MUNRO and T. MURTY. 2003. Tsunami hazard and risk in Canada. *Natural Hazards*, **28** (2-3): 433–461.

DZIEWONSKI, A.; S. BLOCH and M. LANDISMAN. 1969. Technique for the analysis of transient seismic signals. *Bull. Seism. Soc. Am.* **59**: 427–444.

EMERY, W.J. and R.E. THOMSON. 2001. *Data Analysis Methods in Physical Oceanography*. Second and revised edition. Elsevier, New York. 638 pp.

FILLOUX, J.H.; D.S. LUTHER and A.D. CHAVE. 1991. Update on seafloor pressure and electric field observations from the north-central and northeastern Pacific: Tides, infratidal fluctuations, and barotropic flow. In: *Tidal Hydrodynamics*. B.B. Parker (Ed.), J. Wiley, New York. pp. 617– 639.

GEIST, E.L. and S.L BILEK. 2001. Effect of depth-dependent shear modulus on tsunami generation along subduction zones. *Geophys. Res. Lett*. **28:** 1315–1318.

GONZÁLEZ, F.I. and E.A. KULIKOV. 1993. Tsunami dispersion observed in the deep ocean. In: *Tsunamis in the World*. S. Tinti (Ed.), Kluwer Acad. Publ., Dordrecht. pp. 7–16.

HANSON, J.A.; C.L. REASONER and J.R. BOWMAN. 2007. High-frequency tsunami signals of the great Indonesian earthquakes of 26 December 2004 and 28 March 2005. *Bull. Seism. Soc. Am.* **97**: S232–S238.

HONDA, K.; T. TERADA, Y. YOSHIDA and D. ISITANI. 1908. An investigation on the secondary undulations of oceanic tides. *J. College Sci., Imper. Univ. Tokyo*, **24**: 1–113.

KANAMORI, H. 1972. Mechanism of tsunami earthquakes. *Phys. Earth Planet. Int*. **6**: 346–359.

KOWALIK, Z.; W. KNIGHT, T. LOGAN and P. WHITMORE. 2007. The tsunami of 26 December 2004: Numerical modeling and energy considerations. *Pure Appl. Geophys.* **164**: 379–393.

KULIKOV, E.A.; A.B. RABINOVICH, A.I. SPIRIN, S.L. POOLE and S.L. SOLOVIEV. 1983. Measurement of tsunamis in the open ocean. *Marine Geodesy*, **6** (3–4): 311–329.

LOOMIS, H.G. 1966. Spectral analysis of tsunami records from the stations in the Hawaiian Islands. *Bull. Seism. Soc. Am.* **56** (3): 697–713.

MILLER, G.R. 1972. Relative spectra of tsunamis. Hawaii Inst. Geophys. HIG-72-8. 7 pp.

MURTY, T.S. 1977. Seismic Sea Waves - Tsunamis. Bull. Fish. Res. Board Canada 198, 337 pp.

MURTY, T.S. 1992. Tsunami threat to the British Columbia coast. In: Geotechnique and Natural Hazards. BiTech. Publ., Vancouver, BC, pp. 81–89.

OKAL, E.A. 1988. Seismic parameters controlling far-field tsunami amplitudes. *Natural Hazards* **1**: 67–96.

PUGH, D.T. 1987. *Tides, Surges and Mean Sea-Level*. J. Wiley, Chichester, 472 pp.

RABINOVICH, A.B. 1997. Spectral analysis of tsunami waves: Separation of source and topography effects. *J. Geophys. Res*. **102** (C6): 12,663–12,676.

RABINOVICH, A.B. 2005. West coast Vancouver Island, Canada, M_w = 6.7, 2 November 2004, 09:30 UTC, *Tsunami Newsletter*, **37** (1): 5.

RABINOVICH, A.B. and F.E. STEPHENSON. 2004. Longwave measurements for the coast of British Columbia and improvements to the tsunami warning capability. *Natural Hazards*, **32** (3): 313–343.

RABINOVICH, A.B.; R.E. THOMSON and F.E. STEPHENSON. 2006a. The Sumatra Tsunami of 26 December 2004 as observed in the North Pacific and North Atlantic Oceans. *Surveys Geophys.* **27**: 647–677.

RABINOVICH, A.B.; F.E. STEPHENSON and R.E. THOMSON. 2006b. The California Tsunami of 15 June 2005 along the coast of North America. ATMOSPHERE-OCEAN, **44** (4): 415–427.

RABINOVICH, A.B.; L. I. LOBKOVSKY, I. V. FINE, R. E. THOMSON, T. N. IVELSKAYA and E. A. KULIKOV. 2008. Near-source observations and modeling of the Kuril Islands tsunamis of 15 November 2006 and 13 January 2007. *Ad. Geosci.* **14:** 105–116. www.adv-geosci.net/14/105/2008/.

RAPATZ W.J. and MURTY, T.S. 1987. Tsunami warning system for the Pacific coast of Canada. *Marine Geodesy*, **11**: 213–220.

ROGERS, G.C. 1983. Seismotectonics of British Columbia. Ph. D. Thesis, University of British Columbia, Vancouver, 247 pp..

ROGERS, G.C. 1986. Seismic gaps along the Queen Charlotte Fault. *Earthq. Pred. Res.* **4:** 1–11.

SATAKE, K.; K. SHIMAZAKI, Y. TSUJI and K. UEDA. 1996. Time and size of a giant earthquake in Cascadia inferred from Japanese tsunami records of January 1700. *Nature*, **379**: 246–249.

SATAKE, K.; K. WANG and B.F. ATWATER. 2003. Fault slip and seismic moment of the 1700 Cascadia earthquake inferred from Japanese tsunami descriptions. *J. Geophys. Res*. **108** (B11): doi:10.1029/2003JB002521.

SMITH, A.J.; R.D. HYNDMAN, J.F. CASSIDY and K. WANG. 2003. Structure, seismicity, and thermal regime of the Queen Charlotte transform margin. *J. Geophys. Res.* **108** (B11): 2539, doi:10.1029/2002JB002247.

SOLOVIEV, S.L. and CH.N. GO. 1975. *Catalogue of Tsunamis on the Eastern Shore of the Pacific Ocean*. Nauka Publ. House, Moscow, 204 pp. (in Russian; English translation: Canadian Transl. Fish. Aquatic Sci., No. 5078, Ottawa, 293 pp., 1984).

SYNOLAKIS, C.E.; J.-P. BARDET, J.C. BORRERO, H.L. DAVIES, E.A. OKAL, E.A. SILVER, S. SWEET and D.R. TAPPIN. 2002. The slump origin of the 1998 Papua New Guinea tsunami. *Proc. Roy. Soc. London, Ser. A.* **483** (2020): 763–789.

THOMSON, R.E. 1981. Oceanography of the British Columbia Coast. Can. Spec. Publ. Fish. Aquat. Sci. 56, Ottawa, 291 pp.

TITOV, V.V. and C.E. SYNOLAKIS. 1997. Extreme inundation flows during the Hokkaido-Nansei-Oki tsunami. *Geophys. Res. Lett.* **24** (11): 1315–1318.

TITOV, V.V. and F.I. GONZÁLEZ. 1997. Implementation and testing of the Method of Splitting Tsunami (MOST) model. NOAA Tech. Mem. ERL

PMEL-112 (PMEL, Seattle, 1997).

TITOV, V.V.; F.I. GONZÁLEZ, E.N. BERNARD, M.C. EBLE, H.O. MOFJELD, J.C. NEWMAN and A. J. VENTURATO. 2005a. Real-time tsunami forecasting: Challenges and solutions. *Natural Hazards*, **35**: 41–58.

TITOV, V.V.; A.B. RABINOVICH, H. MOFJELD, R.E. THOMSON and F.I. GONZÁLEZ. 2005b. The global reach of the 26 December 2004 Sumatra tsunami. *Science*, **309**: 2045–2048.

WHITMORE, P.M. 2003. Tsunami amplitude prediction during events: A test based on previous tsunamis. *Sci. Tsunami Hazards*, **21**: 135–143.

WIGEN, S.O. 1983. Historical studies of tsunamis at Tofino, Canada. In: *Tsunamis – Their Science and Engineering*. K. Iida and T. Kawasaki (Eds), Terra Sci. Publ. Comp., Tokyo, Japan, pp. 105–119.

WIGEN S.O. and W.R.H. WHITE. 1964. Tsunami of March 27–29, 1964. West coast of Canada. Report, Dept of Mines and Technological Surveys, 1–6 August 1964.